New Neurons Follow the Flow of Cerebrospinal Fluid in the Adult Brain

Kazunobu Sawamoto,[1,4,5]* Hynek Wichterle,[3] Oscar Gonzalez-Perez,[1] Jeremy A. Cholfin,[1,2] Masayuki Yamada,[6] Nathalie Spassky,[1] Noel S. Murcia,[7] Jose Manuel Garcia-Verdugo,[8] Oscar Marin,[9] John L. R. Rubenstein,[2] Marc Tessier-Lavigne,[10] Hideyuki Okano,[5] Arturo Alvarez-Buylla[1]*

In the adult brain, neuroblasts born in the subventricular zone migrate from the walls of the lateral ventricles to the olfactory bulb. How do these cells orient over such a long distance and through complex territories? Here we show that neuroblast migration parallels cerebrospinal fluid (CSF) flow. Beating of ependymal cilia is required for normal CSF flow, concentration gradient formation of CSF guidance molecules, and directional migration of neuroblasts. Results suggest that polarized epithelial cells contribute important vectorial information for guidance of young, migrating neurons.

The structure and function of the central nervous system depends on precisely controlled movements of young neurons (*1*). Perhaps one of the most complex and far-reaching forms of neuronal migration occurs in the adult brain: Neuroblasts born in the subventricular zone (SVZ), next to the walls of the lateral ventricles, migrate to the olfactory bulb where they differentiate into local interneurons (*2*–*5*). In rodents, these young neurons first migrate in the SVZ, where they form a complex network of interconnected chains (*6*). Young neurons then join the rostral migratory stream (RMS), which leads them into the core of the olfactory bulb. It has been proposed that

[1]Department of Neurological Surgery and Developmental and Stem Cell Biology Program, [2]Nina Ireland Laboratory of Developmental Neurobiology, University of California San Francisco, San Francisco, CA 94143, USA. [3]Department of Pathology, Columbia University, New York, NY 10032, USA. [4]Bridgestone Laboratory of Developmental and Regenerative Neurobiology, [5]Department of Physiology, Keio University School of Medicine, Tokyo 160-8582, Japan. [6]Central Institute for Experimental Animals, Kawasaki, Kanagawa 216-0001, Japan. [7]Rainbow Center for Childhood Polycystic Kidney Disease, Department of Pediatrics, Case Western Reserve University, Cleveland, OH 44106–6003, USA. [8]University of Valencia, Burjassot-46100, Spain. [9]Instituto de Neurosciencias de Alicante of the Consejo Superior de Investigaciones Científicas (CSIC) and University Miguel Hernández, 03550 Sant Joan d'Alacant, Alicante, Spain. [10]Genentech, Inc., South San Francisco, CA 94080–4990, USA.

*To whom correspondence should be addressed. E-mail: sawamoto@sc.itc.keio.ac.jp (K.S.); abuylla@stemcell.ucsf.edu (A.A.B.)

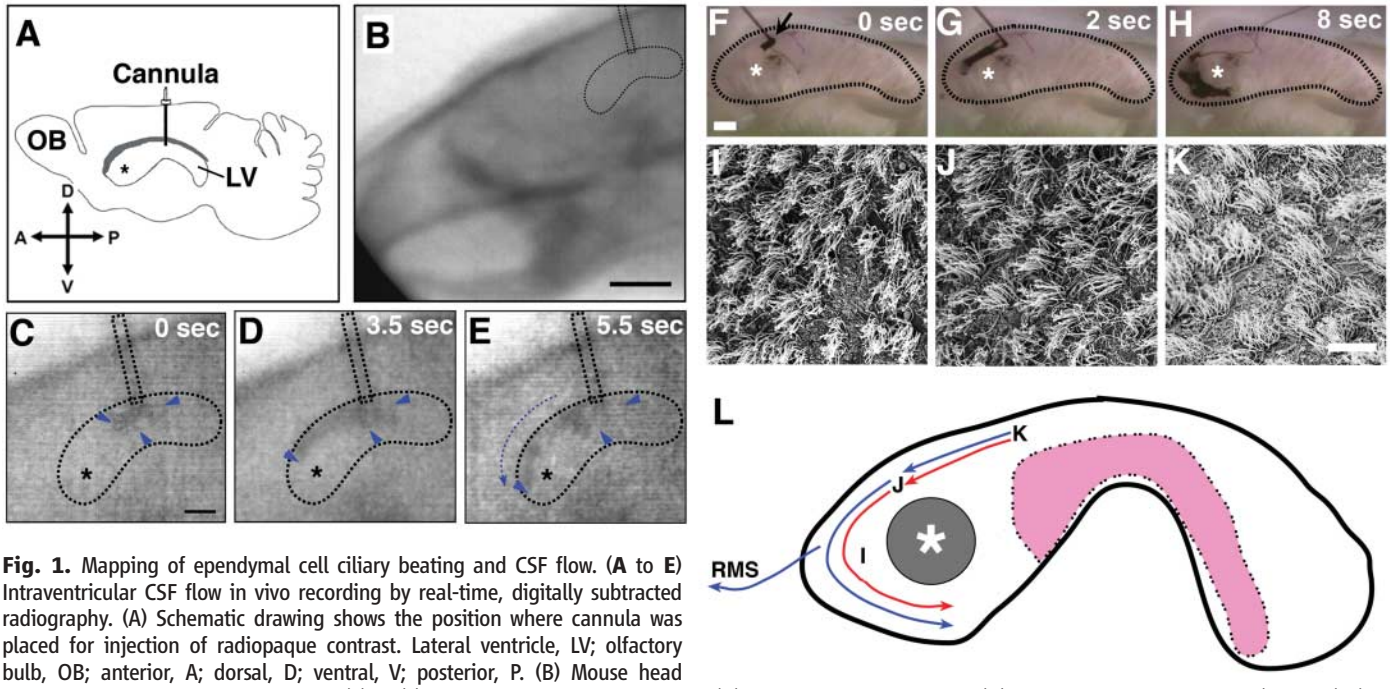

Fig. 1. Mapping of ependymal cell ciliary beating and CSF flow. (**A** to **E**) Intraventricular CSF flow in vivo recording by real-time, digitally subtracted radiography. (A) Schematic drawing shows the position where cannula was placed for injection of radiopaque contrast. Lateral ventricle, LV; olfactory bulb, OB; anterior, A; dorsal, D; ventral, V; posterior, P. (B) Mouse head radiogram before injection of contrast. (C) to (E) Serial radiograms were taken every 0.33 s. (C) At 0 s, (D) at 3.5 s, and (E) at 5.5 s. (See movie S1.) Dashed lines denote the lateral ventricle and cannula placement. Note how the contrast (arrowheads) moves along a dorsal corridor and then turns ventrally around the anterior horn (dashed arrow). The mean time of contrast movement to reach the anterior tip of the ventricle from the injection site (–1.0 mm relative to bregma) was 6.3 ± 0.8 s (SD) ($n = 6$). The site of the wall adhesion is marked by an asterisk. (**F** to **H**) Ependymal flow revealed by India ink placed [(F), arrow] onto exposed surface of the lateral wall of the lateral ventricle ($n = 6$). Note how ink moves along a dorsal corridor (G) and then turns ventrally (H) around the wall adhesion (asterisk). (See movie S2.) (**I** to **L**) Scanning electron micrographs showing orientation of ependymal cilia at various locations on the lateral wall of the lateral ventricle as indicated in (L). Cilia beat ventrally in the anterior part of the anterior horn (I), beat anteriorly in the dorsal anterior horn (J), and beat anterodorsally in the intermediate region dorsal to the choroid plexus (K). (L) Note how the direction of CSF flow (red) is similar to cell migration pattern (blue) (see Fig. 2) around the wall adhesion (asterisk). Scale bars: (B), 0.5 cm; (C) to (E), 0.15 cm; (F) to (H), 1 mm; (I) to (K), 10 μm. Pink denotes the location of choroid plexus.

Slit proteins expressed in septum (*7*, *8*) and choroid plexus (*9*) are the relevant chemorepulsive factors. Septum and choroid plexus are separated from the SVZ by the lateral ventricle filled with CSF and by the epithelial lining of the lateral ventricle, the ependyma. It is not understood how CSF guidance molecules reach the SVZ and form gradients in the adult brain. The ependyma is polarized with oriented bundles of motile cilia protruding into the lateral ventricle lumen (*10*, *11*). Coordinated, whiplike motion of epithelial cilia has been proposed to direct flow of mucosa and fluids in the trachea, oviduct, and ventricles (*12*).

Pattern of ependymal flow in the lateral ventricle. To record intraventricular CSF flow in vivo, we injected a contrast agent into the caudal lateral ventricle of adult mice (n = 6), which was detected by real-time fluoroscopy. The contrast agent injected into the ventricle moved rostrally along a dorsal corridor into the anterior horn and then ventrally around the adhesion area (Fig. 1, A to E; movie S1). Magnetic resonance imaging (MRI) (n = 10) of $MnCl_2$ secreted from the choroid plexus revealed similar CSF movement (fig. S2). To directly correlate the flow of CSF with the planar polarity of ependymal cells, we deposited a small amount of India ink onto the exposed surfaces of dissected walls of lateral ventricles (n = 6). The pattern of ink flow, generated by the beating ependymal cilia, paralleled that of CSF flow observed in vivo (Fig. 1, F to H; movie S2). Furthermore, the orientation of cilia beating observed live under the light microscope or, after fixation, by scanning electron microscopy was similar to the patterned flow observed in vivo and in vitro (Fig. 1, I to K) (*11*). These results indicate that ciliary beating and planar polarity of ependymal cells generate directed currents of fluid adjacent to the ventricular wall.

Neuroblast migration parallels CSF flow. There is a remarkable similarity between the direction of CSF flow and the organization of the network of chains of migrating neuroblasts in the SVZ (*6*) (Fig. 2A). To determine the orientation of migrating neuroblasts at different locations in the SVZ, we labeled neuroblasts by focal injections of a retrovirus encoding alkaline phosphatase. Direction of migration was inferred from the average orientation of the leading process (598 cells in 25 animals), a reliable indicator of SVZ neuroblast migration (*13*, *14*) (Fig. 2). As expected, of 184 cells in the RMS, 81.0% were oriented in the direction of the olfactory bulb. Likewise, in the dorsal SVZ, of 303 cells, 60.7% pointed in the direction of the RMS, an orientation equivalent to that of the CSF flow on the ventricular surface in this region. It was noteworthy that, in the anterior SVZ, only 20.7% of neuroblasts (of 111) pointed dorsally toward the RMS, whereas 45.9% were oriented in the ''reverse'' direction ($P < 0.01$, chi-square analysis) (Fig. 2, B and C), which parallels the flow of CSF (Fig. 1). Thus, the orientation of neuroblast migration correlates with the flow of CSF rather than with the relative position of the olfactory bulb.

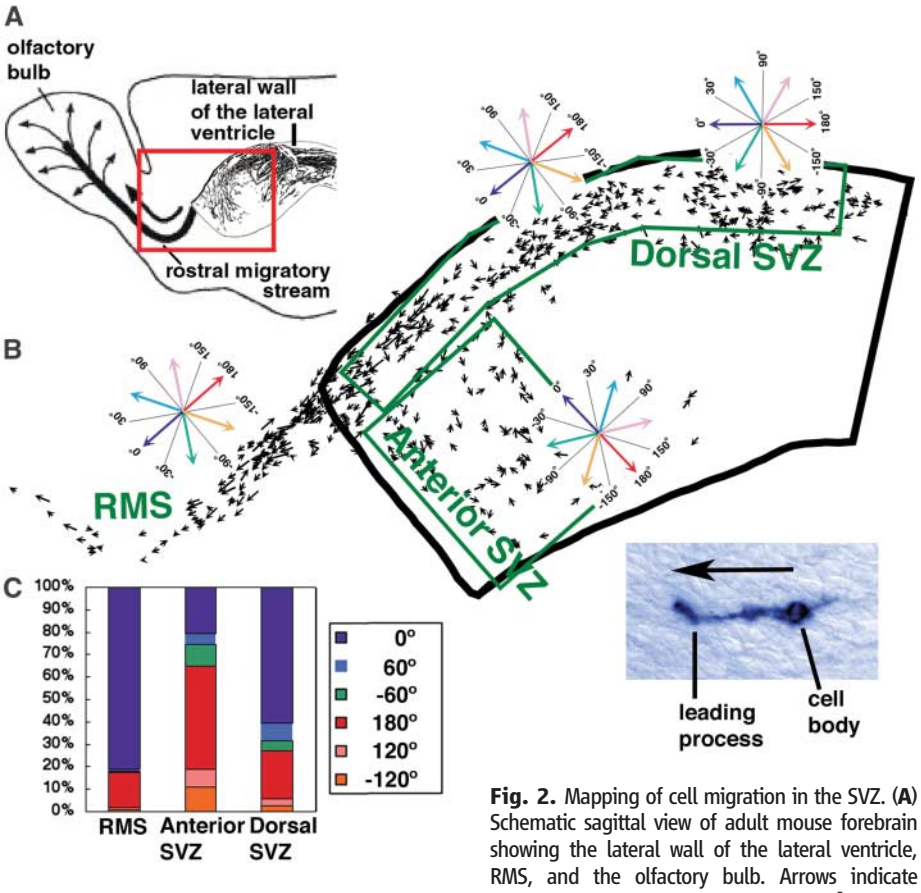

Fig. 2. Mapping of cell migration in the SVZ. (**A**) Schematic sagittal view of adult mouse forebrain showing the lateral wall of the lateral ventricle, RMS, and the olfactory bulb. Arrows indicate direction of migration. Camera lucida drawing of the chains of neuroblasts in the SVZ is included [modified from (*6*)]. (**B**) Composite map of the direction of cell migration (from 25 animals) in the SVZ (delineated by green rectangles) and RMS. Each black arrow in the map indicates the orientation and length of the leading process of individual cells. Neuroblasts were labeled with a retrovirus encoding alkaline phosphatase (see inset for example). (**C**) Quantification of cell migration. The orientation of the leading process of each cell was used to determine the percentage of cells oriented in the direction of the olfactory bulb (defined as 0°) [see compasses in (B)]. In the dorsal SVZ and in the RMS, 0° was defined in the direction of the olfactory bulb and parallel to the longitudinal array of chains. Cells pointing in the reverse direction were considered oriented at 180°. For the anterior SVZ, 0° orientation was defined dorso-anteriorly in the direction of the longitudinal array of chains leading to the olfactory bulb. Note in the histogram how the majority of cells in the dorsal SVZ and RMS have a 0° orientation (toward the olfactory bulb). In contrast, the majority of cells in the anterior SVZ are pointing ventrally (180°) away from the RMS and olfactory bulb. The total numbers of cells counted in each region: RMS, 184; anterior SVZ, 111; and dorsal SVZ, 303.

Ependymal flow is required for neuroblast orientation. To determine whether ependymal ciliary beating is required for normal SVZ cell migration, we studied *Tg737*^{orpk} mutant mice (*15*, *16*). These mice carry a hypomorphic allele for Polaris, which is essential for normal ciliogenesis. As a consequence, these animals have hydrocephalus, develop polycystic kidney disease, and show disruptions in left-right asymmetry (*15*, *16*). Ependymal cells cover the walls of the ventricles in *Tg737*^{orpk} mutant mice, but these cells had few, short, irregular cilia compared with ependymal cells in the wild type (fig. S3, A and B). Most of the mutant cilia were not motile (movie S3), and occasional motile cilia were not sufficient to produce CSF flow (movie S2). Fluoroscopic imaging in vivo also showed lack of normal CSF flow in *Tg737*^{orpk} animals (fig. S1, movie S1).

Neuroblasts stained with antibody against the polysialylated form of the neural cell adhesion molecule (PSA-NCAM) were found in the SVZ of *Tg737*^{orpk} mice, and these cells became organized into chains similar to those observed in wild-type mice (Fig. 3, A and B). Strikingly, however, chains in

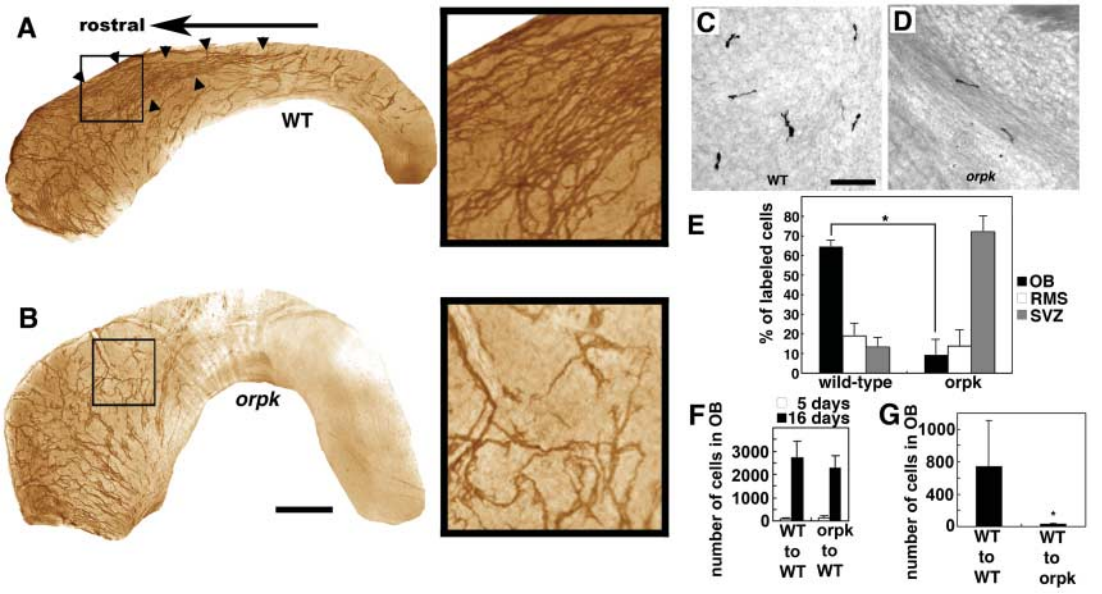

Fig. 3. Cell migration defects in the *Tg737*^{orpk} mutant. (**A** and **B**) Whole mounts of the lateral walls of the lateral ventricle stained with antibody against PSA-NCAM. A well-organized longitudinal array of chains (arrowheads) was observed in the wild-type brain (WT) (A) but not in the *Tg737*$^{orpk/orpk}$ mutant (B). Higher magnification views of the dorsal region marked by squares (A) and (B) are shown in the insets to the right. (**C** to **E**) Normal cilia are required for rostral migration of endogenous neuroblasts. Sagittal sections of wild-type (C) and *Tg737*^{orpk} (D) olfactory bulbs 5 days after injection of alkaline phosphatase–encoding retrovirus into the SVZ. (E) The number of alkaline phosphatase^{+} cells (means ± SD) reaching the olfactory bulb in the *Tg737*$^{orpk/orpk}$ mice was significantly smaller than in the wild type ($P = 0.0004$, *t* test). Total number of cells counted: wild type, 396 ($n = 3$); mutant, 112 ($n = 3$). (**F**) *Tg737*$^{orpk/orpk}$ mutant neuroblasts can migrate normally in the wild-type brain. SVZ cells from wild-type or *Tg737*$^{orpk/orpk}$ mutant mice carrying GFP were grafted into the SVZ of wild-type brains. (See fig. S4.) The histogram shows the number of GFP^{+} cells (means ± SD) in the olfactory bulbs 5 days ($n = 4$) and 16 days ($n = 4$) after transplantation. No significant difference was observed ($P = 0.7763$ at day 5 and 0.422 at day 16, *t* test). (**G**) Wild-type neuroblasts failed to migrate normally in the *Tg737*$^{orpk/orpk}$ mutant brain. GFP-labeled SVZ cells from wild-type mice were grafted into the SVZ of wild-type and *Tg737*$^{orpk/orpk}$ mutant mice. (See fig S4.) The histogram shows the number of GFP^{+} cells in the olfactory bulbs 5 days after transplantation (means ± SD) ($n = 4$). The number of wild-type cells reaching the olfactory bulb in the *Tg737*$^{orpk/orpk}$ brain was significantly smaller than in the wild type to wild type transplantation controls ($P = 0.048$, *t* test). OB, olfactory bulb. Scale bars: (A) and (B), 1 mm; (C) and (D), 50 μm.

Tg737^{orpk} mice were severely disoriented compared with those of wild-type mice. This derailing was most noticeable in the dorsal SVZ, where in wild-type animals the majority of chains were oriented longitudinally. In *Tg737*^{orpk} mice, chains in this region were oriented in multiple directions, including many chains oriented perpendicular to their normal longitudinal orientation (Fig. 3, A and B). Chain disorientation was observed in all *Tg737*^{orpk} mice analyzed ($n = 3$). Proliferating and pyknotic cells in the SVZ and RMS of *Tg737*^{orpk} mice were found in locations and in numbers similar to those of wild-type animals (fig. S3). However, *Tg737*^{orpk} mice develop hydrocephalus because of the lack of normal CSF flow, and this ventricular expansion could have induced chain disorientation. As a control, we induced obstructive hydrocephalus in wild-type mice by partial surgical obstruction of the aqueduct of Sylvius, a manipulation that did not affect the pattern of ink flow on the lateral ventricular wall. In these animals, the orientation of chains was not affected (*17*), which suggests that hydrocephalus alone was not the cause of disoriented chains.

To study the migration of neuroblasts from the SVZ into the olfactory bulb in *Tg737*^{orpk} mice, we labeled cells in the SVZ with an alkaline phosphatase–encoding retrovirus (Fig. 3, C to E). By 5 days after injection, 64.6% of the alkaline phosphatase–positive cells had reached the olfactory bulb in the wild-type littermates ($n = 3$). In contrast, in the *Tg737*^{orpk} mutant ($n = 3$), only 9.3% of the cells were found in the olfactory bulb, and 73.4% remained in the SVZ. Of the few neuroblasts ($n = 18$) that reached the RMS and olfactory bulb in the *Tg737*^{orpk} mutant, 77.8% were oriented in the forward direction, which suggests that normal ependymal cilia are required for proper migration of neuroblasts along the SVZ network, but not in the RMS or olfactory bulb. *Tg737*^{orpk} mutant neuroblasts carrying green fluorescent protein (GFP) were able to migrate normally to the olfactory bulb when grafted into wild-type SVZ ($n = 4$) (Fig. 3F; fig. S4, A to D). In contrast, few GFP^{+} wild-type cells grafted into the *Tg737*^{orpk} mutant SVZ ($n = 4$) reached the olfactory bulb (Fig. 3G; fig. S4, E and F). These grafting experiments indicated that *Tg737*^{orpk} mutation disturbs directional neuroblast migration in a manner that is not cell autonomous. Although we cannot totally exclude an indirect effect from chronic hydrocephalus or other defects in *Tg737*^{orpk} mutant animals on SVZ neuroblast migration, the above experiments strongly suggest that the absence of appropriate ependymal flow in *Tg737*^{orpk} mutant animals results in disorientation of SVZ neuroblast migration.

Ependymal flow is required for formation of chemorepulsive gradients in the SVZ. How might guidance cues be presented to migrating SVZ neuroblasts in vivo? CSF is secreted mainly from the choroid plexus, located in the caudal regions of the lateral ventricle (Fig. 1L). The choroid plexus is a source of chemorepulsive factors, including members of the Slit family, which influence SVZ cell migration (*9*, *18*). Ependymal cells allow access of CSF proteins or exogenous tracers to the underlying brain parenchyma (*19*, *20*). To determine how Slit proteins in CSF become distributed in vivo, we infused a recombinant Slit2–alkaline phosphatase fusion protein (Slit2-AP) into the caudal lateral ventricle close to the choroid plexus ($n = 5$) (Fig. 4, A to F). Slit2-AP protein was found not only on the surface of the ependymal layer, but also within the SVZ (Fig. 4, C and D). Importantly, the alkaline phosphatase signal was found in a gradient along the dorsal SVZ, with the highest signal in the caudal region (Fig. 4D), and progressively weaker signal was detected rostrally (Fig. 4, B and C). Remarkably, the gradient corresponds to the ventricular region of greatest forward CSF flow and to the SVZ area in which neuroblasts form longitudinal arrays of chains and migrate predominantly in a rostral direction (Fig. 4A). In contrast, the normal concentration

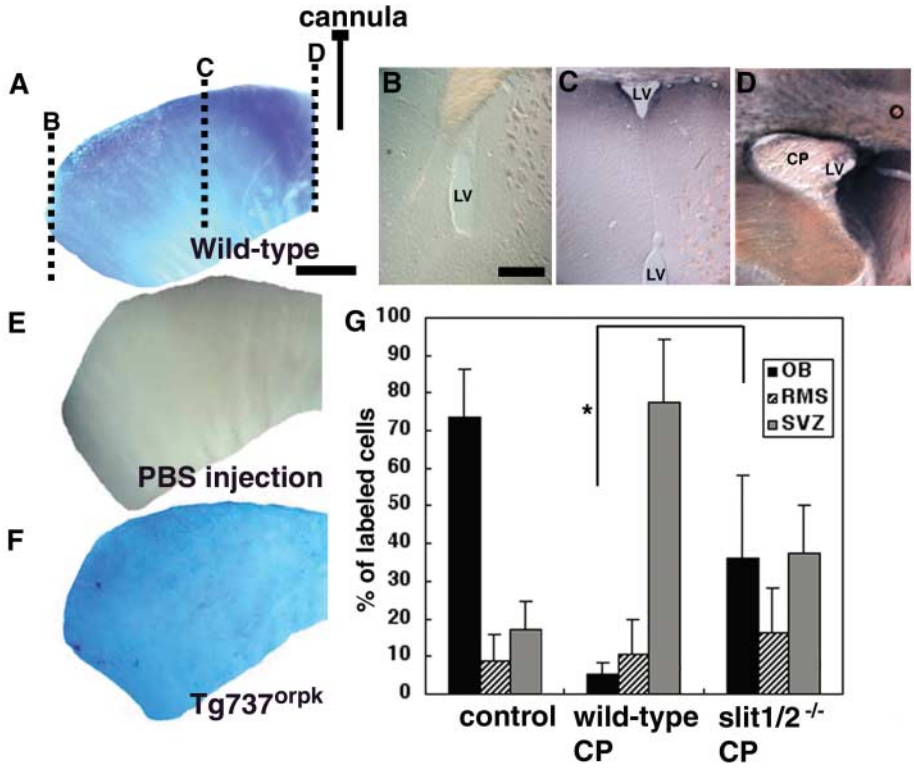

Fig. 4. Slit2-AP concentration gradient formation in the SVZ. (**A** to **F**) The Slit2-AP fusion protein was infused into the caudal lateral ventricle close to the choroid plexus in wild-type [(A) to (D)] (n = 5) and *Tg737*^{orpk} mutant (F) (n = 3) brains. Whole mounts of the lateral ventricular wall (anterior horn) [(A), (E), and (F)] or coronal sections [(B) to (D)] were stained for alkaline phosphatase enzyme activity 24 hours after the beginning of infusion. (E) Phosphate-buffered saline injection resulted in no signal (n = 1). (B) to (D) correspond to three different rostrocaudal levels of an infused brain sectioned in the coronal plane as shown approximately by the dotted lines in (A). Slit2-AP was deposited in a gradient, with the highest alkaline phosphatase activity detected in the caudal and dorsal SVZ. (F) Injection of Slit2-AP into the caudal lateral ventricle of Tg737^{orpk} mutants did not result in the formation of this gradient. (**G**) *Slit1/2* mutant (n = 5) or wild-type (n = 4) choroid plexuses were transplanted dorsal to the RMS. (See fig. S5.) As a control, meninges (n = 4) were grafted in the same location. One month later, alkaline phosphatase–encoding retrovirus was injected into the SVZ. Five days after injection, alkaline phosphatase$^+$ cells (means ± SD) were counted. In controls, most of the alkaline phosphatase–labeled cells have reached the olfactory bulb, with few cells remaining in the SVZ and RMS. The pattern was reversed in the choroid plexus–grafted (CP) animals; most of the cells failed to reach the olfactory bulb and remained in the SVZ. This repulsive effect of the choroid plexus graft was partially reversed in the Slit1/2 mutant (P = 0.0068, t test). OB, olfactory bulb. Scale bars: (A), (E), and (F), 1 mm; (B) to (D), 0.5 mm.

gradient did not form when Slit2-AP was injected into the lateral ventricle of *Tg737*^{orpk} mutants (n = 3) (Fig. 4F). These results indicate that CSF flow is necessary for the formation of the Slit2 gradient in the SVZ in vivo.

Anterior grafts of choroid plexus disrupt rostral neuroblast migration. To test whether disruption of a concentration gradient of chemorepulsive factors secreted by choroid plexus affects directional neuroblast migration in vivo, we transplanted a fragment of wild-type or *Slit1/2* mutant choroid plexus anteriorly, just dorsally to the RMS (fig. S5Q). RMS morphology, retroviral injection, and cell transplantation indicated that wild-type choroid plexus anterior to the SVZ inhibits most, if not all, of the rostral migration of the neuroblasts into the olfactory bulb (fig. S5). The number of retrovirally labeled alkaline phosphatase$^+$ cells reaching the olfactory bulb was significantly greater in animals with a grafted *Slit1/2* mutant choroid plexus (n = 6) than in animals that received a similar-size, wild-type choroid plexus graft (n = 8) (Fig. 4G). This indicates that Slit proteins contribute to the choroid plexus's repulsive activity in vivo. Interestingly, animals with *Slit1/2* mutant choroid plexus grafts had fewer alkaline phosphatase$^+$ cells in the olfactory bulb than mice that received no grafts or control grafts of meninges (Fig. 4G), which suggests that additional factors expressed in choroid plexus, such as Slit3 (*21*), may be responsible for the residual choroid plexus repulsive activity.

Our results suggest that the planar polarity of ciliated ependymal cells is essential for the formation of chemorepulsive–factor gradients that guide neuroblast migration in the adult brain. Previous work, which implicated nodal cilia in the determination of left-right asymmetry (*22*), indicates that polarized ciliated cells contribute important vectorial information for body plan development. The present work suggests that polarized epithelia and motile cilia in the brain serve as important conveyors of directional information for neuronal migration.

References and Notes

1. O. Marin, J. L. Rubenstein, *Annu. Rev. Neurosci.* **26**, 441 (2003).
2. J. Altman, *J. Comp. Neurol.* **137**, 433 (1969).
3. M. B. Luskin, *Neuron* **11**, 173 (1993).
4. C. Lois, A. Alvarez-Buylla, *Science* **264**, 1145 (1994).
5. S. O. Suzuki, J. E. Goldman, *J. Neurosci.* **23**, 4240 (2003).
6. F. Doetsch, A. Alvarez-Buylla, *Proc. Natl. Acad. Sci. U.S.A.* **93**, 14895 (1996).
7. H. Hu, U. Rutishauser, *Neuron* **16**, 933 (1996).
8. W. Wu *et al.*, *Nature* **400**, 331 (1999).
9. H. Hu, *Neuron* **23**, 703 (1999).
10. M. R. Del Bigio, *Glia* **14**, 1 (1995).
11. T. Yamadori, K. Nara, *Scan. Electron Microsc.* **1979** (3), 335 (1979).
12. B. Alberts, *Molecular Biology of the Cell* (Garland, New York, ed. 3, 1994).
13. H. Wichterle, J. M. Garcia-Verdugo, A. Alvarez-Buylla, *Neuron* **18**, 779 (1997).
14. B. T. Schaar, S. K. McConnell, *Proc. Natl. Acad. Sci. U.S.A.* **102**, 13652 (2005).
15. P. D. Taulman, C. J. Haycraft, D. F. Balkovetz, B. K. Yoder, *Mol. Biol. Cell* **12**, 589 (2001).
16. N. S. Murcia *et al.*, *Development* **127**, 2347 (2000).
17. O. Gonzalez-Perez and A. Alvarez-Buylla, unpublished observations.
18. K. T. Nguyen-Ba-Charvet *et al.*, *J. Neurosci.* **24**, 1497 (2004).
19. R. B. Aird, *Exp. Neurol.* **86**, 342 (1984).
20. M. W. Brightman, *J. Cell Biol.* **26**, 99 (1965).
21. W. Yuan *et al.*, *Dev. Biol.* **212**, 290 (1999).
22. Y. Okada, S. Takeda, Y. Tanaka, J. C. Belmonte, N. Hirokawa, *Cell* **121**, 633 (2005).
23. We thank J. Aruga for the p*APTag2-Slit2* vector; G. Rougon for the PSA-NCAM antibody; C. Yaschine for editorial help; and A. Chédotal, Y. Uchiyama, T. Uemura, F. Murakami, S. Yonemura, and members of our laboratories for insightful discussions and encouragement. This work was supported by Bridgestone Corporation, a gift from Frances and John Bowes, and grants from NIH (NS 28478 and HD 32116), The Ministry of Education, Culture, Sports, Science and Technology, Japan Science and Technology Agency (CREST), Mitsui Life Social Welfare Foundation, and the Ministry of Health, Labor and Welfare.

Supporting Online Material

www.sciencemag.org/cgi/content/full/1119133/DC1
Materials and Methods
Figs. S1 to S5
References
Movies S1 to S3

22 August 2005; accepted 3 January 2006
Published online 12 January 2006;
10.1126/science.1119133
Include this information when citing this paper.